Elastica solutions in viscous fingering. The nonlinear Saffman-Taylor instability

E. Álvarez-Lacalle,* J. Ortín, and J. Casademunt
Dept. ECM, Universitat de Barcelona, Av. Diagonal 647, E-08028, Barcelona, Spain
(Dated: December 27, 2018)

A family of exact stationary solutions of the Saffman-Taylor problem with finite surface tension is reported both in channel and circular geometry (with rotation). The solutions, which relate to Euler's *elastica* problem for the shapes of bending rods, are identified as an unstable branch which bifurcates from the marginal mode of the planar interface and ends up at a topological singularity. This implies a *nonlinear* nature of the Saffman-Taylor instability, and defines a generic bifurcation scenario for a class of interfacial instabilities. Making use of a new experimental procedure to prepare arbitrary initial conditions we have been able to check quantitatively the nonlinear instability implied by our analytical results.

PACS numbers: 47.20.Ma,47.20.Ky,47.54.+r

arXiv:nlin/0304041v1 [nlin.PS] 23 Apr 2003

The Saffman-Taylor (ST) instability [1, 2] has been instrumental during several decades as a paradigm of interfacial pattern formation in nonequilibrium extended systems, both as a simple example of morphological instability and as a nontrivial but solvable problem of pattern selection.

More recently the ST problem is playing a central role in the analytical study of the nonlinear *dynamics* of unstable interfaces, remarkably due to the availability of explicit time–dependent solutions in the case of zero surface tension. The singular character of the surface tension perturbation has been shown to have dramatic effects, not only on the selection of the stationary ST finger, but also on the dynamics [3, 4]. However, while asymptotic analysis for small surface tension has proven fruitful, typical fingering patterns emerging from the linear instability, have dimensionless surface tension of order 1 since the spatial scale is set by the balance between capillary and viscous forces. Unfortunately, the problem with finite surface tension has remained very elusive to analytical treatment. A systematic weakly nonlinear theory has been recently introduced in this case for the early nonlinear regime [5]. However, no exact solutions are known, except for those due to Kadanoff [6] which apply to a configuration very different from the traditional ST arrangement [1]. In this letter we report for the first time on a class of exact stationary solutions with finite surface tension, for both channel and radial geometry (the latter with centrifugal forcing).

Exact solutions to nonlinear problems are generally scarce, although the explicit knowledge of nontrivial exact solutions of prototype nonlinear problems is indeed a valuable resource to elucidate issues that may hold some degree of universality. Specifically, the explicit knowledge of our exact solutions shows that the ST instability (and similarly the Mullins–Sekerka and other related instabilities) is in fact a *nonlinear* one, in the sense that linearly stable perturbations may become unstable if their amplitude is larger than a finite threshold, which can now be determined in terms of the physical parameters [7]. The pursuit of this idea yields a novel bifurcation scenario which is arguably generic for a class of interfacial instabilities: a subcritical unstable branch of steady solutions bifurcates from the trivial (planar) solutions, but ends at a topological singularity (where the solution ceases to make physical sense due to interface pinchoff) rather than turning into a newly stable branch. A quantitative check of this scenario and its observable implications will be carried out experimentally in a Hele–Shaw (HS) cell, using a new procedure to prepare initial conditions *à la carte*.

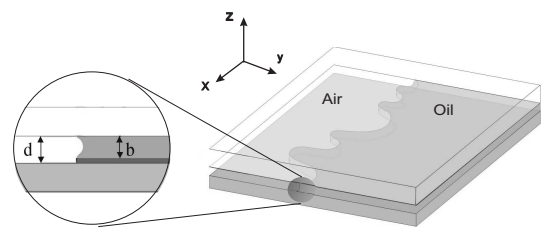

FIG. 1: Sketch of a rectangular Hele–Shaw cell. The gap step used to prepare arbitrary initial conditions is also sketched.

We consider a rectangular HS cell, made of two parallel plates separated by a small gap b (Fig. 1). In the generic case a less viscous fluid 1 (air) displaces a more viscous fluid 2 (oil), as the latter is withdrawn from one side at velocity V_∞. We consider the evolution of the interface position $\vec{r}(s,t)$ as a function of the interface arclength s and time t, given in the vortex–sheet formulation due to Trygvasson and Aref [8]. The velocity field is decomposed into a curl free part and a divergence free part, respectively, $\vec{v} = \vec{w} + \vec{u}$. In the channel geometry $\vec{w}$ can be absorbed in a change of reference frame, so in a co–moving frame the evolution of the interface position is given by $\dot{\vec{r}}(s,t)\cdot\hat{n} = \vec{U}\cdot\hat{n}$, where

$$\vec{U}(s,t) = \frac{1}{2\pi} P \int \frac{\hat{z}\times(\vec{r}(s,t)-\vec{r}(s',t))}{\mid \vec{r}(s,t)-\vec{r}(s',t)\mid^2}\gamma(s',t)ds'. \quad (1)$$

In this equation P denotes the principal value of

the integral and $\gamma = 2A(\hat{\mathbf{U}} \cdot \hat{\mathbf{s}}) + 2C\hat{\mathbf{y}} \cdot \hat{\mathbf{s}} + 2D\kappa_s$ is the vorticity. The coefficients are given by $A = (\mu_2 - \mu_1) / (\mu_2 + \mu_1)$ (dynamic viscosity contrast), $C = \left(b^2/12\right) g \left(\rho_2 - \rho_1\right) / \left(\mu_2 + \mu_1\right) + AV_\infty$ (including the possibility of a gravity component g in the $\hat{y}$ direction), $D = \left(b^2/12\right) \sigma / \left(\mu_2 + \mu_1\right)$. In these expressions ρ_1, ρ_2 are the densities of the fluids, σ their interfacial tension, and κ_s the derivative of the in–plane local curvature of the interface.

The key observation of our analysis is that the requirement of having a vortex–free flow to yield stationary interface shapes can be achieved by a purely geometrical condition since, from Eq. (1), $\gamma = 0$ is a sufficient condition for $\vec{U} = 0$, and inserting $\vec{U} = 0$ in the definition of the vorticity yields a simple ODE for the interface shape. This defines a nontrivial class of stationary solutions. The form of the ODE will depend on the geometry of the specific setup and the boundary conditions.

In the channel geometry, in terms of the angle θ between the normal direction and the y axis, the condition $\gamma = 0$ yields a nonlinear ODE of the form

$$B\theta_{ss} + \sin\theta = 0, \tag{2}$$

where $B = D/C$. Note that, if s is interpreted as time, this is the well known pendulum equation. The corresponding uniparametric family of solutions, parametrized by p, reads

$$\theta = 2\arcsin\left(p \;\; sn\left(\frac{s - s_0}{\sqrt{B}}, p\right)\right), \tag{3}$$

where $sn(y, p)$ is the Jacobi elliptic function [9]. Examples of the corresponding stationary interface shapes are shown in Fig. 2. Note that the solutions given in Eq. (3) are independent of A, and that surface tension, though necessary, only sets the spatial scale. Increasing values of p define periodic interfaces of decreasing wavelength λ. For a limiting value $p = p_l$ the solution $h(x)$ presents a topological singularity, implying an interface pinchoff. Beyond p_l the curves obtained have no longer physical meaning.

In the present context, the ubiquitous pendulum equation, a landmark in nonlinear science, provides an appealing analogy with the so called Euler's *elastica* problem [10], originally proposed by Bernoulli in 1691, i.e. the determination of the shape of thin bending rods as minimizers of the elastic energy $E = \int \kappa^2(s) ds$ under certain constraints. This problem is of current relevance in the context of stiff biopolymers (DNA, F–actin). In particular, the shape of the pinchoff solution in Fig. 2 coincides exactly with the 'racquet' solution of Ref. [11]. Although the ST problem is non–variational, the *elastica* solutions of the ST problem arise as equilibrium solutions that balance exactly the competing capillary and viscous forces. Contrary to Euler's *elastica* solutions, however, our solutions are expected to be unstable, as will be shown later.

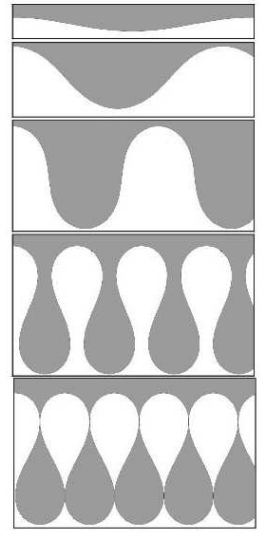

FIG. 2: Exact stationary solutions of the ST problem with nonzero surface tension, in channel geometry.

For the purely gravity–driven case these solutions do not travel and resemble those of pendant drops [12], since they now result from a balance between capillary and hydrostatic pressure.

This procedure can be generalized to radial geometry for a rotating Hele–Shaw cell [13, 14], in which centrifugal and capillary forces can be exactly balanced. In polar coordinates, the condition of zero vorticity now reads

$$\kappa_\phi - \frac{\left(\rho_2 - \rho_1\right)\Omega^2}{\sigma} r r_\phi = 0, \tag{4}$$

where Ω is the angular velocity of the cell and the inner fluid 2 is more dense than the outer fluid 1. A sample of the resulting stationary shapes is shown in Fig. 3. In the presence of fluid injection, however, viscous pressure and capillary pressure can only be balanced for a given time, and do not yield stationary solutions.

The class of solutions here reported has a clear interpretation in the framework of bifurcation theory, and therefore may be claimed to encompass some degree of universality. It corresponds to the unstable branch of solutions which can be anticipated to originate at the bifurcation point of the ST instability, where the planar solution exchanges stability. This branch is shown in Fig. 4. The bifurcation is subcritical, as required by the fact that the growth is not saturated by nonlinearities. Such branch of solutions must occur in similar problems featuring unsaturated growth but, in general, the question about how this branch is continued in the deeply nonlinear regime remains open. This can only be answered analytically with an exact solution. The answer for the ST problem is that the branch ends up at a topological singularity, associated with the occurrence of interface

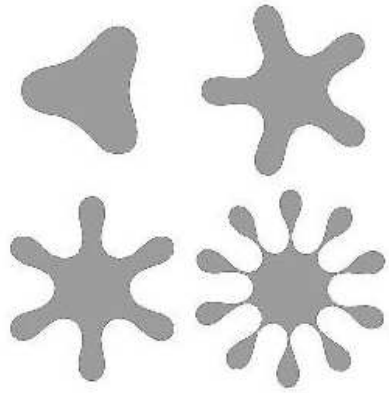

FIG. 3: Exact stationary solutions with nonzero surface tension, in a rotating circular Hele–Shaw cell without fluid injection.

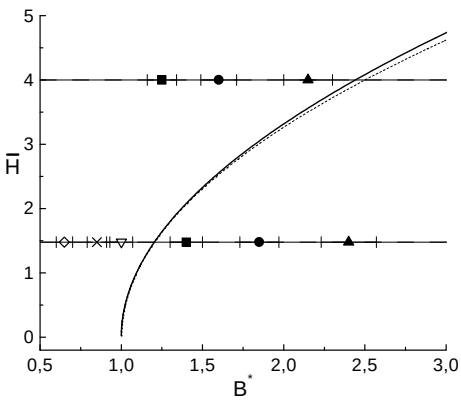

FIG. 4: The distance H between the maximum and the minimum displacement of the interface is plotted vs. B, in scaled variables $\bar{H} = H\,(2\pi/\lambda)$, $B^* = B\,(2\pi/\lambda)^2$, up to $B^* = 3$. The branch of exact unstable solutions (subcritical) is represented by a solid thick line. The branch would continue up to $B^* = 23.9$, where the interface pinchoff occurs. The dashed line is the weakly nonlinear approximation obtained from Eq. (5). The different initial conditions used in the experiments are also shown with different symbols.

pinchoff. The scenario should be valid also for solidification problems, at least for small Péclet number [15].

To show that our solutions constitute the continuation of the above unstable branch that originates at the bifurcation point, it suffices to carry out a weakly nonlinear analysis. We consider a finite cell of width L in which air displaces a viscous fluid ($A = 1$). Following Ref. [5], we get for the amplitude δ_1 of the first unstable mode:

$$\dot{\delta_1} = (1 - B)\delta_1 + \frac{3}{2} \mid \delta_1 \mid^2 \delta_1, \qquad (5)$$

where for simplicity we have used $C = 1$ and $L = \lambda = 2\pi$. We have found that our exact solutions coincide indeed

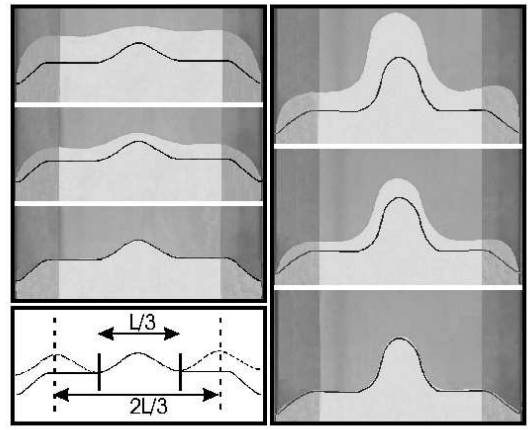

FIG. 5: Snapshots of two experiments for two different initial conditions, showing respectively the decay and the growth of two finite amplitude perturbations of the planar interface, under identical experimental conditions. Time increases upwards in both sequences. We also sketch how the initial conditions are designed in order to minimize boundary effects. The whole channel width is shown, but the quantitative analyses are performed for the central, non-shaded strip of width $2L/3$.

with the stationary solutions ($\dot{\delta_1} = 0$) of this weakly nonlinear approximation for small amplitudes, as shown in Fig. 4.

The presence of a branch of unstable *elastica* solutions in the bifurcation diagram implies a *nonlinear* ST instability, according to which, a linearly stable configuration may grow unstable for finite amplitude perturbations above a threshold determined by the branch of stationary solutions shown in Fig. 4.

In order to probe experimentally this prediction, we have carried out a series of experiments in a horizontal H–S cell of size $750 \times 250 \times 15$ ($L \times W \times T$ in mm), separated by a brass frame carefully machined to provide a gap spacing $b = 0.500 \pm 0.015$ mm between the plates. The cell is originally filled with a silicone oil Rhodorsil 47V10 (dynamic viscosity $\mu = 8.4 \pm 0.2$ cP and density $\rho = 0.93 \pm 0.01$ g/cm^3 at 20°C). In the experiment the oil is withdrawn at a constant rate from one side of the cell, using a syringe pump, and is progressively displaced by the air entering from the other side.

Essential to these experiments is the ability to generate initial conditions of prescribed shapes. To this aim we have developed a procedure that exploits the sensitivity of capillary pressure to slight gap thickness variations. By making the gap of the Hele–Shaw cell on the side of the displaced fluid slightly narrower than on the displacing fluid, and the step between the two regions follow a prescribed shape, as shown in Fig. 1, we can hold the interface at the desired initial shape until injection is started [16].

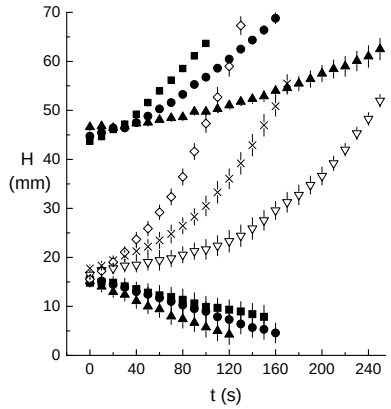

FIG. 6: Time evolution of the measured maximum–to–minimum distance of the interface for different experiments. The experimental parameters are indicated in Fig. 4 for the corresponding symbols. All the interfaces decay or grow depending on whether they are respectively below or above the branch of solutions depicted in Fig. 4.

The initial conditions investigated experimentally are shown in Fig. 5. The central part, of lateral size $L/3$, corresponds to an exact stationary solution with $\lambda = L/3$. This is continued on each side with a flat section of size $L/6$, and terminated with a receding section, also of size $L/6$ that meets the side walls perpendicularly. This particular form of the initial condition is designed to minimize the influence of the boundaries, which is critical in these experiments.

The results of two typical experiments are presented in Fig. 5. The experiment on the left has been prepared with an amplitude of the initial condition $\bar{H} = 1.5$, which corresponds to $B^* = 1.2$ in the branch of stationary solutions of Fig. 4. On the right the amplitude is $\bar{H} = 4.0$, which corresponds to $B^* = 2.5$. Both experiments, however, have been carried out with the same nominal injection, $Q = 65$ ml/h (i.e. $B^* = 1.7$). According to the bifurcation diagram represented in Fig. 4, the first initial condition should decay to the (linearly stable) flat interface, and the second initial condition should grow towards a new stationary solution, the ST finger. This is exactly what we observe, as shown in Fig. 5.

We have checked that our experimental conclusions are robust by running the experiment for different injection rates using the same two initial conditions of Fig. 5. The corresponding B^* are shown in Fig. 4. The growth or decay of the interface amplitude H with time in these experiments is shown in Fig. 6. The results provide firm experimental evidence that the branch of unstable *elastica* solutions in the bifurcation diagram separates two distinct dynamic regions: on the left of the curve the finite–amplitude perturbations are amplified towards the ST finger, and on the right of the curve the perturbations decay.

In summary, we have found a class of exact solutions of the longstanding ST problem which has dynamical implications in interfacial problems in a variety of disciplines. The identification of a class of solutions with those of the *elastica* problem for bending rods (also related to the solutions of the pendulum equation), puts this problem in contact with a broad spectrum of fields in mathematics, physics and biology.

We acknowledge the financial support of the DGES (MCyT, Spain) under project BXX2000-0638-C02-02, and of the DURSI (Generalitat de Catalunya) under project SGR-2000-00433. EAL is supported by a grant of the DURSI.

* Electronic address: enric@ecm.ub.es

[1] P.G. Saffman and G.I. Taylor, Proc. Roy. Soc. London Ser. A **245**, 312 (1958).
[2] D. Bensimon, L. Kadanoff, S. Liang, B.I. Shraiman, and C. Tang, Rev. Mod. Phys. **58**, 977 (1986).
[3] J. Casademunt and F.X. Magdaleno, Phys. Rep. **337**, 1 (2000).
[4] E. Pauné, M. Siegel, and J. Casademunt, Phys. Rev. E **66**, 46205 (2002); E. Pauné, PhD thesis (2002).
[5] E. Álvarez–Lacalle, J. Casademunt, and J. Ortín, Phys. Rev. E **64**, 016302 (2001); Phys. Rev. E (2003), in press.
[6] L.P. Kadanoff, Phys. Rev. Lett. **65**, 2986 (1990).
[7] A different nonlinear instability was already reported for the ST problem modified by the addition of surfactants by H. Guo, D.C. Hong, and D.A. Kurtze, Phys. Rev. Lett. **69**, 1520 (1992); Phys. Rev. E **51**, 4469 (1995).
[8] G. Trygvasson and H. Aref, J. Fluid Mech. **136**, 1 (1983).
[9] M. Abramowitz and I.A. Stegun (Eds.), *Handbook of Mathematical Functions with Formulas, Graphs, and Mathematical Tables*, 9th printing. New York: Dover, 1972, pp. 567–626.
[10] L. Euler, *Curvarum Maximi Minimive Proprietate Gaudentium Inventio Nova ac Facilis*, 1744.
[11] B. Schnurr, F.C. MacKintosh, and D.R.M. Williams, Europhys. Lett. **51**, 279 (2000); B. Schnurr, F. Gittes, and F.C. MacKintosh, Phys. Rev. E **65**, 061904 (2002).
[12] C.S. Riera, E. Risler, Nonlinearity **15**, 1843 (2002).
[13] L.W. Schwartz, Phys. Fluids A **1**, 167 (1989).
[14] L. Carrillo, F.X. Magdaleno, J. Casademunt, and J. Ortín, Phys. Rev. E **54**, 6260 (1996).
[15] D. Jasnow, J. Viñals, Phys. Rev. A **40**, 3864 (1989).
[16] In our experiment the gap thickness is modified by attaching a thin film of polyethylene (Alkor-Decor, 0.1 mm thickness) to the region of the bottom plate to be covered initially by the oil. One end of the plastic film is cut carefully with the profile of the desired initial condition. The small difference in capillary pressure across the interface suffices to hold the interface still, following the profile of the film step.